

Supporting Information

Colorimetric and Ratiometric Fluorescent Chemodosimeter for Selective Sensing of Fluoride and Cyanide Ion: Tuning Selectivity in Proton Transfer and C-Si Bond Cleavage

Ajit Kumar Mahapatra^{*},^a Saikat Kumar Manna,^a Bhaskar Pramanik,^b Kalipada Maiti,^a Sanchita Mondal,^a Syed Samim Ali^a and Debasish Mandal^c

^a Department of Chemistry, Indian Institute of Engineering Science and Technology, Shibpur, Howrah-711103, West Bengal, India,

Email: akmahapatra@rediffmail.com, Fax: +913326684564

^b Indian Institute of Science Education and Research, Kolkata, India.

^c Institute of Chemistry, The Hebrew University of Jerusalem, 91904 Jerusalem, Israel.

1. ^1H NMR spectrum of LHSi (400 MHz, CDCl_3):

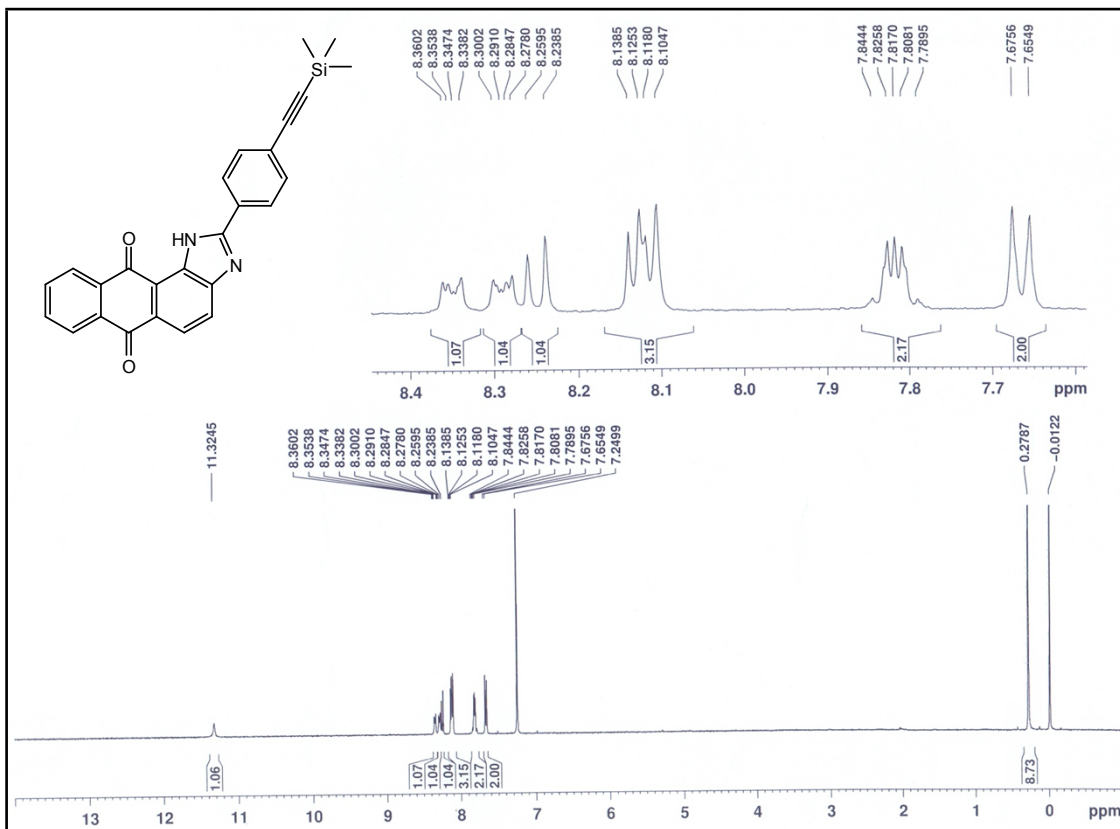


Figure S1: ^1H NMR spectrum of LHSi in CDCl_3 solution.

2. ^{13}C NMR spectrum of LHSi (400 MHz, CDCl_3):

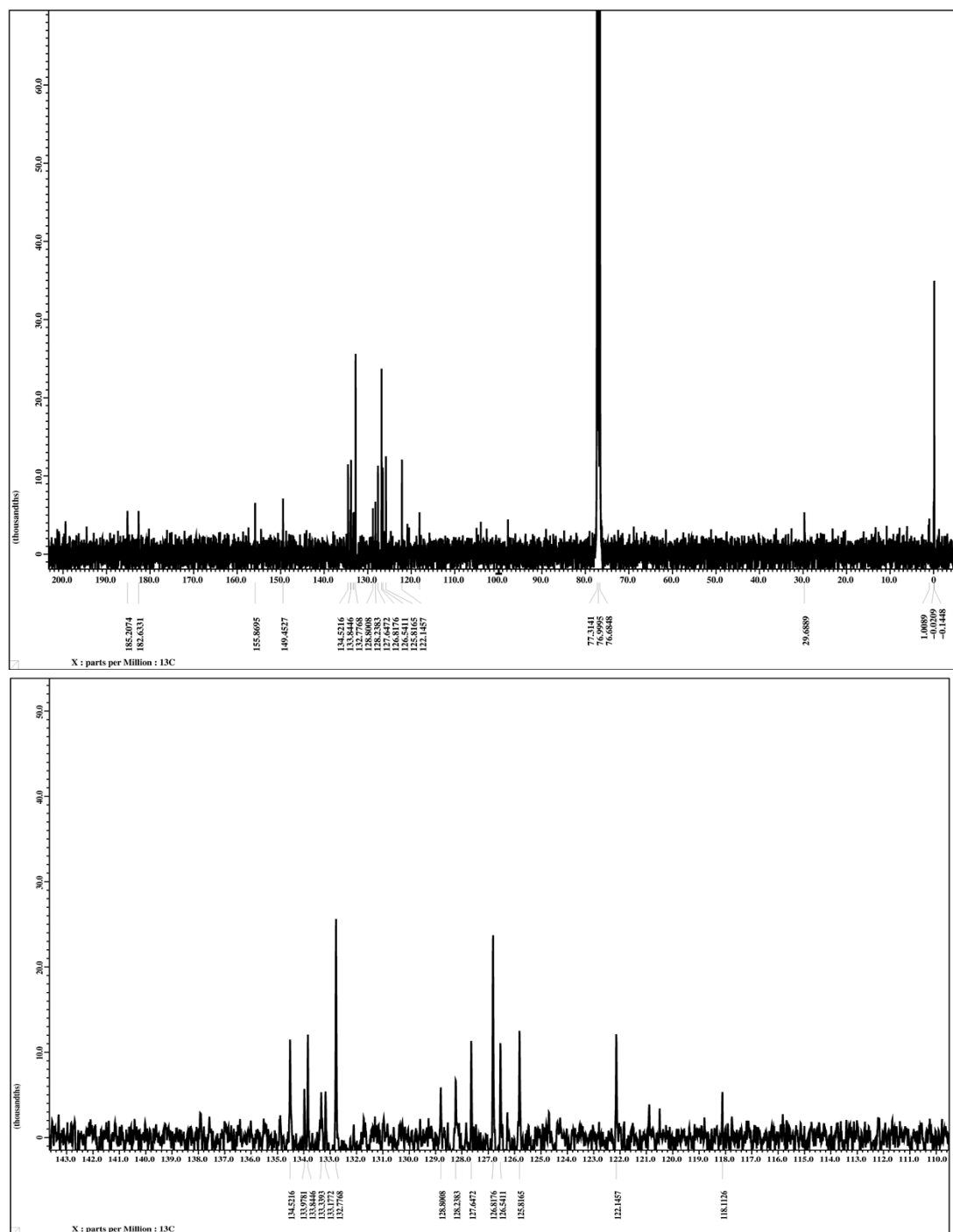


Figure S2: ^{13}C NMR spectrum of LHSi in CDCl_3 solution.

3. Mass spectrum of LHSi:

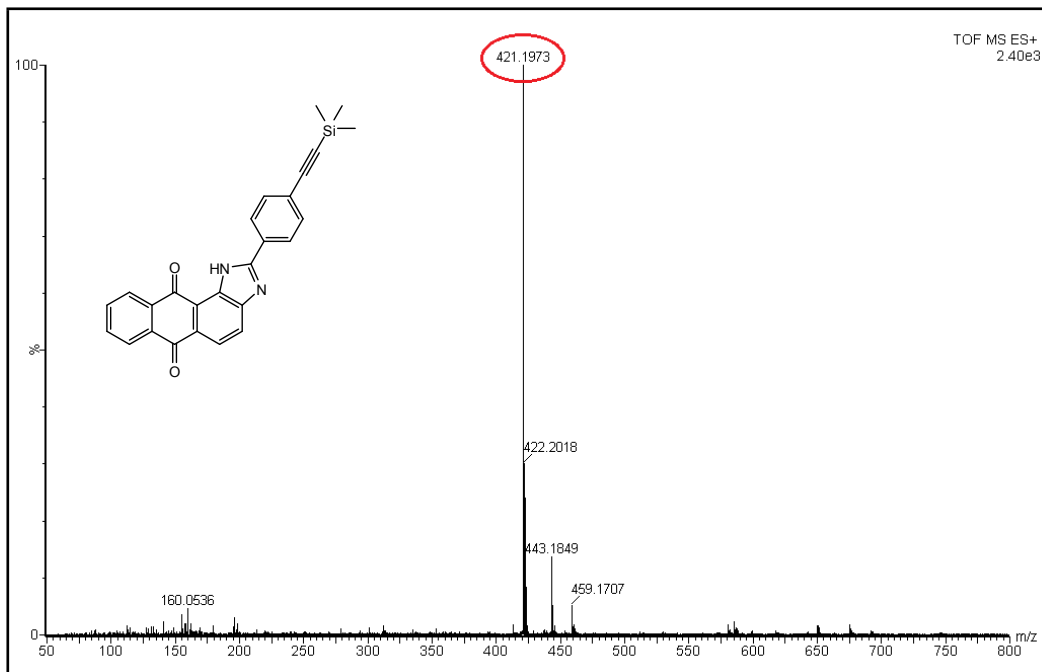


Figure S3: ESI-MS of LHSi .

4. UV-Vis and fluorescence spectra of LHSi in presence of TBAOH:

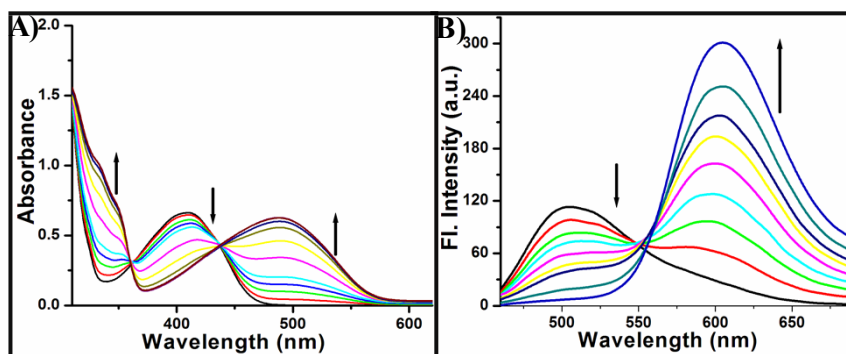


Figure S4: (A) Absorption and (B) fluorescence spectral changes of LHSi ($c = 4 \times 10^{-5}$ M) upon addition of TBAOH in THF solution.

5. ^1H NMR titration of LHSi in presence of TBAF:

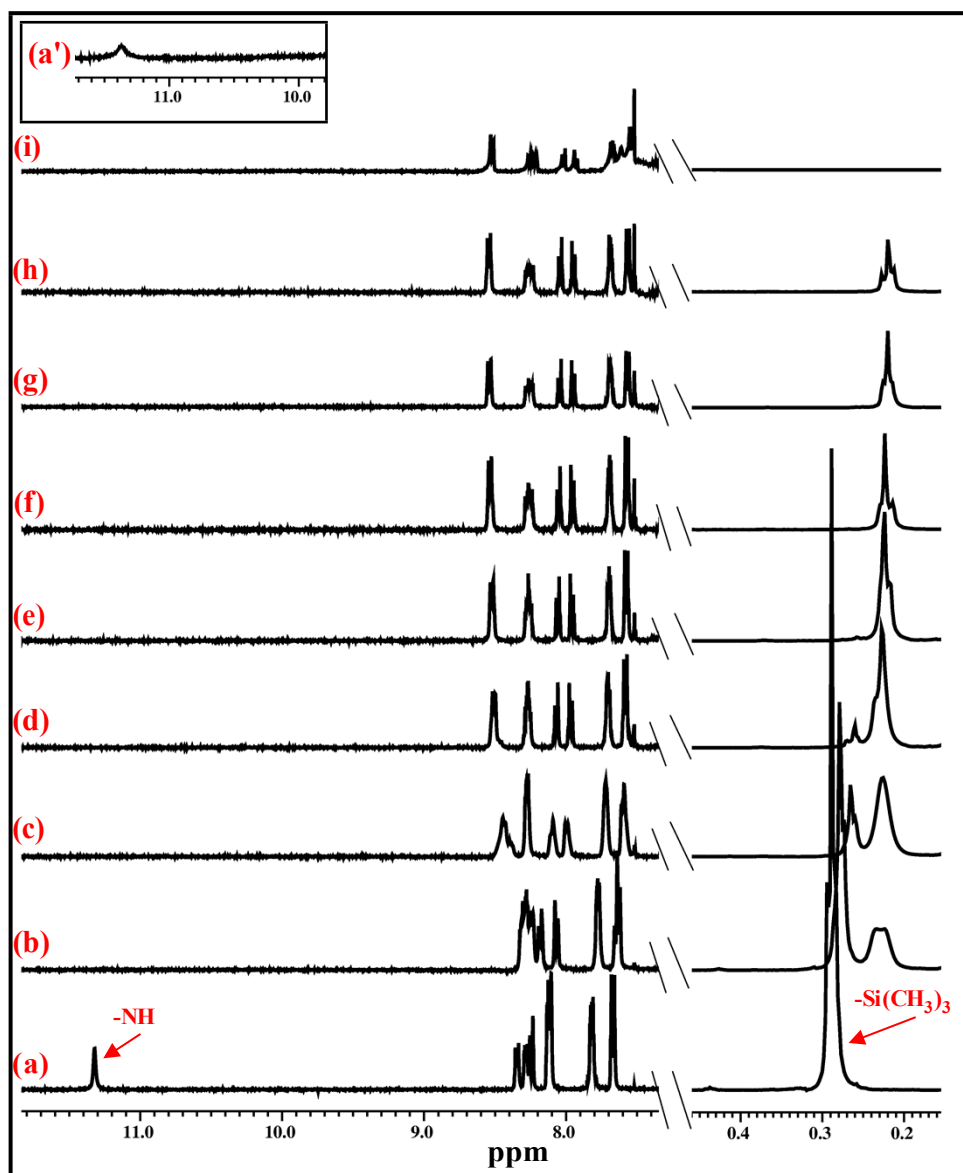


Figure S5: Partial ^1H NMR (400 MHz) spectra of LHSi in CDCl_3 in (a) the absence and the presence of (a') 0.5 (inset), (b) 1.0, (c) 1.5, (d) 2.0, (e) 2.5, (f) 3.0, (g) 4.0, (h) 5.0, (i) 10.0 equiv of TBAF.

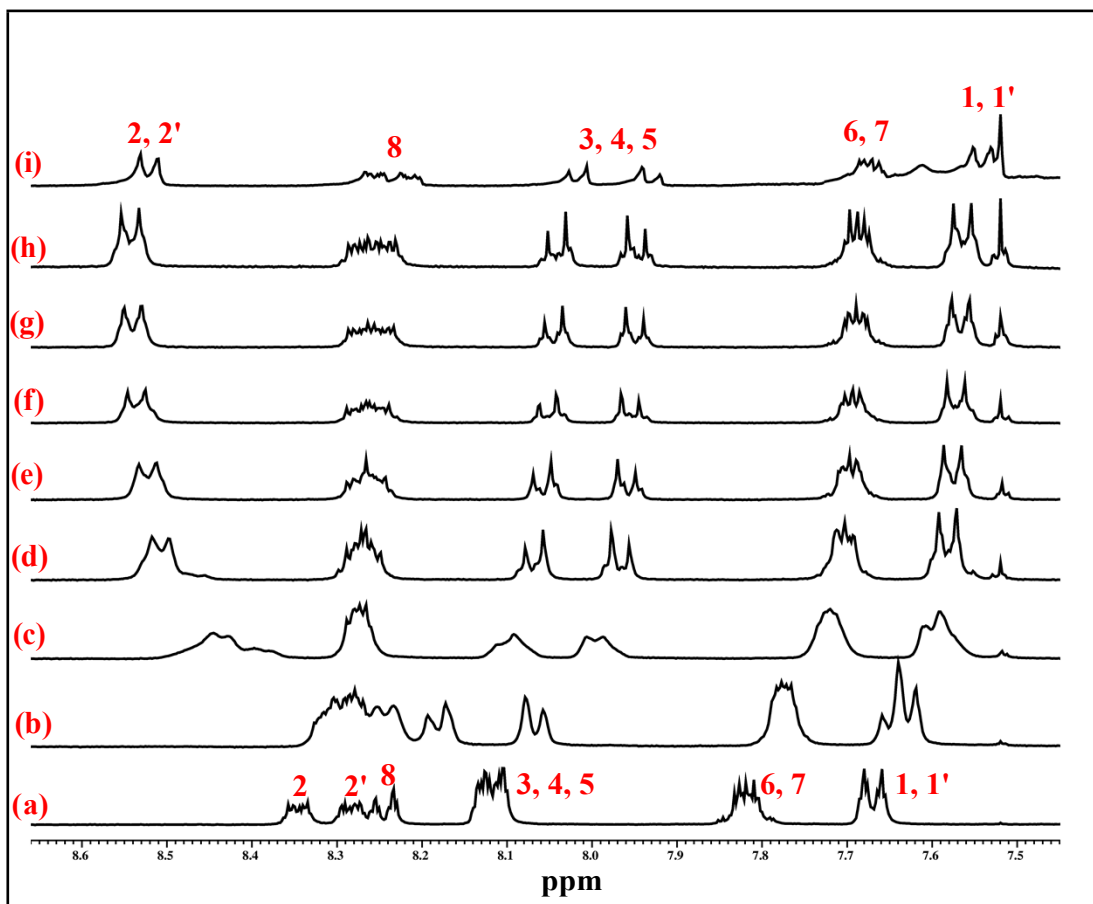
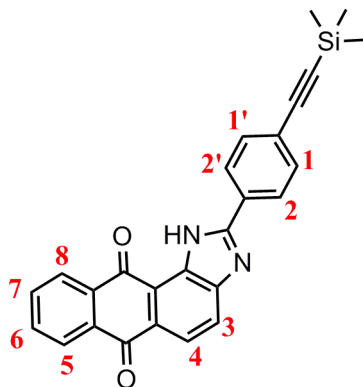


Figure S6: Partial expanded ^1H NMR (400 MHz) spectra of aromatic region of **LHSi** in CDCl_3 in (a) the absence and the presence of (b) 1.0, (c) 1.5, (d) 2.0, (e) 2.5, (f) 3.0, (g) 4.0, (h) 5.0, (i) 10.0 equiv of TBAF.

6. ^1H NMR titration of LHSi in presence of TBACN:

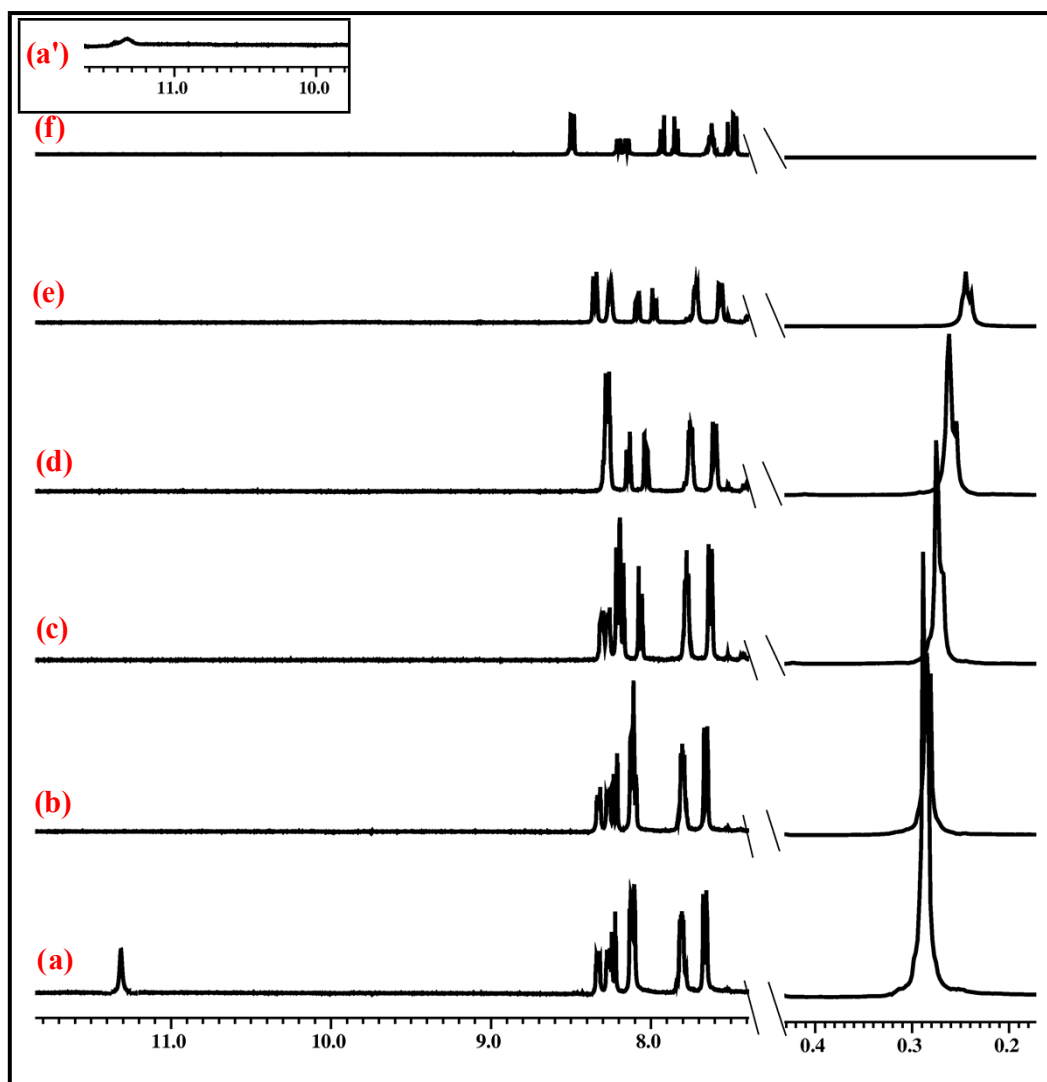


Figure S7: Partial ^1H NMR (400 MHz) spectra of **LHSi** in CDCl_3 in (a) the absence and the presence of (a') 0.5 (inset), (b) 1.0, (c) 1.5, (d) 2.0, (e) 4.0, (f) 10.0 equiv of TBACN.

7. Mass spectrum of LHSi + TBAF:

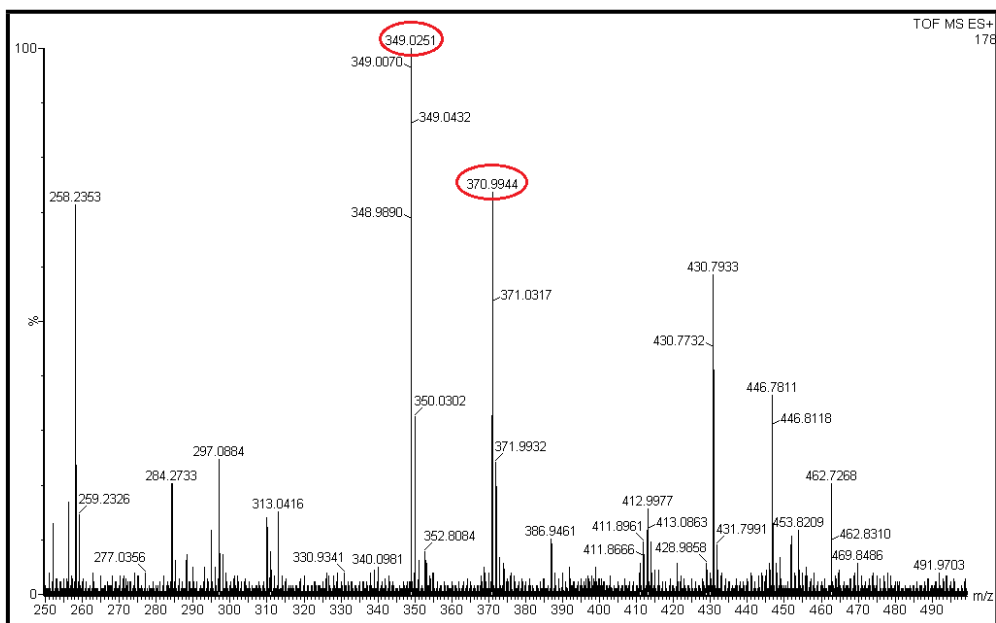


Figure S8: ESI-MS spectral evidence for desilylation of LHSi on treatment with TBAF.

8. Mass spectrum of LHSi + TBACN:

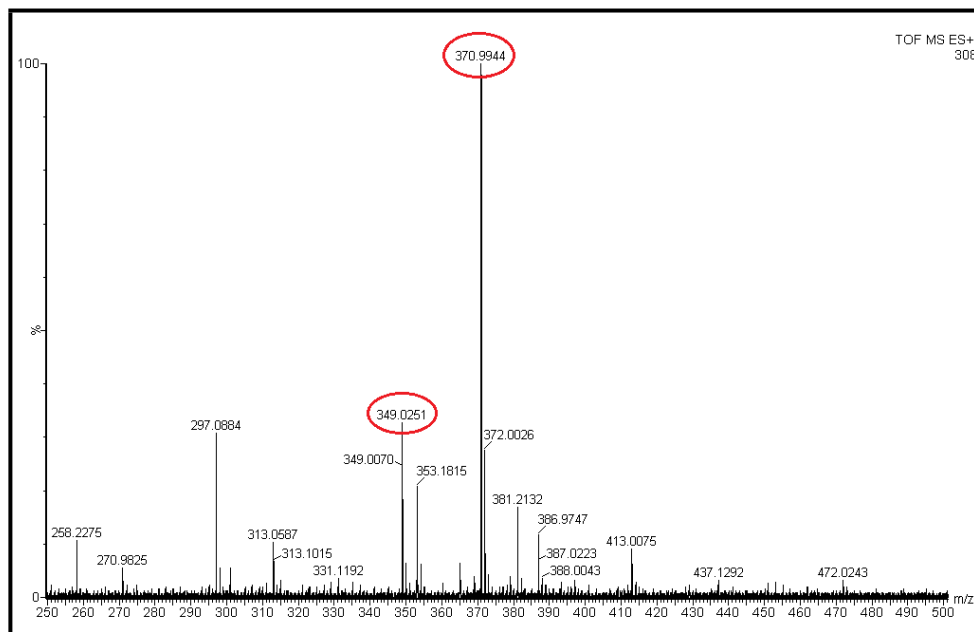


Figure S9: ESI-MS spectral evidence for desilylation of LHSi on treatment with TBACN.

9. Mass spectrum of LHSi on treatment with Hg^{2+} as a counteraction with fluoride:

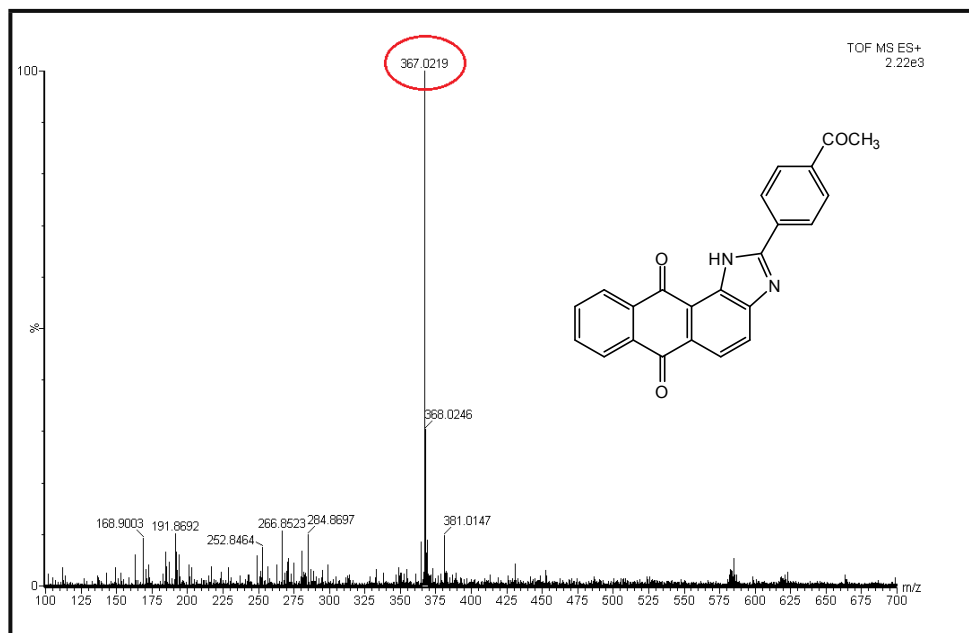


Figure S10: ESI-MS of LHSi on treatment with Hg^{2+} as a counteraction with fluoride.

10. Computational Study:

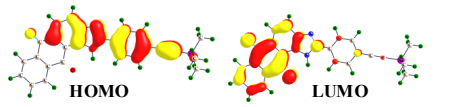
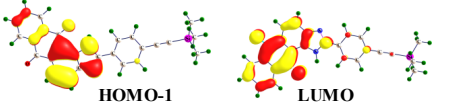
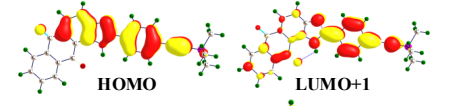
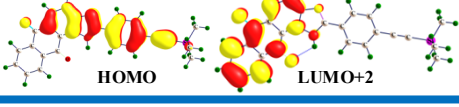
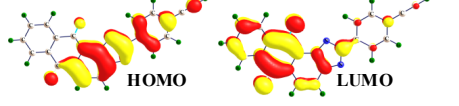
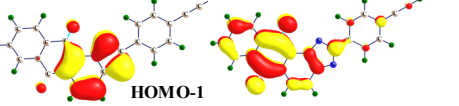
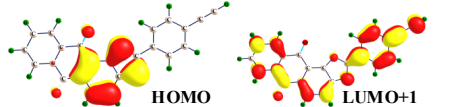
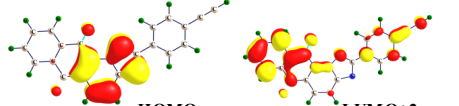
	Molecular orbital	Electronic contribution of transition
LHSi		HOMO → LUMO (97.3%)
		HOMO-1 → LUMO (98.0%)
		HOMO → LUMO+1 (90.2%)
		HOMO → LUMO+2
L⁻		HOMO → LUMO (83.5%)
		HOMO-1 → LUMO (13.8%)
		HOMO → LUMO+1 (93.5%)
		HOMO → LUMO+2

Figure S11. Molecular orbitals and electronic contribution of the relevant excitations of **LHSi** and **L⁻**.

Table S1. Selected electronic excitation energies (eV), oscillator strengths (f), main configurations, and CI Coefficients of the low-lying excited states of **LHSi** and **L⁻**. The data were calculated by TDDFT//B3LYP/6-31+G(d) based on the optimized ground state geometries.

Molecules	Electronic Transition	Excitation Energy ^a	f ^b	Composition ^c	(composition) %
LHSi	S ₀ → S ₁	2.6362 eV 470 nm	0.3664	H → L	97.3
	S ₀ → S ₃	3.1090 eV 398.79 nm	0.9420	H-1 → L	98.0
	S ₀ → S ₈	3.8881 eV 318.88 nm	1.0016	H → L + 1 H → L + 2	90.2
	S ₀ → S ₁₆	4.6356 eV 267.46 nm	0.2809	H-1 → L + 2 H → L + 3	85.1
L⁻	S ₀ → S ₂	2.3657 eV 524.09 nm	0.3417	H-1 → L H → L	13.8 83.5
	S ₀ → S ₆	3.4742 eV 356.87 nm	0.5410	H → L+1 H → L+2	93.5
	S ₀ → S ₈	3.6764 eV 337.24 nm	0.2539	H-1 → L+3	87.3

[a] Only selected excited states were considered. The numbers in parentheses are the excitation energy in wavelength. [b] Oscillator strength. [c] H stands for HOMO and L stands for LUMO.